Microwave Transmission through Gallium Single Crystals*†

Robert F. Milligan‡
Department of Physics and Astronomy, University of Rochester, Rochester, New York 14627
(Received 8 March 1973)

The transmission of 9.23-GHz radiation through thin gallium plates at 1.3 °K is studied as a function of external magnetic field strength and orientation in the three principal planes. The transmitted signal consists primarily of sample-thickness dependent Gantmakher-Kaner oscillations arising from conduction electrons with both effective and ineffective trajectories. Certain of the ineffective-electron signals have either amplitude dips at cyclotron resonance or odd harmonic content, features which are expected when the surface scattering is specular. One cyclotron-phase-resonance branch was also observed in the thinnest sample. In addition to measuring the value of the product $m^*\langle v_H\rangle$ for each branch, $\langle v_H\rangle$ was obtained for certain cases.

I. INTRODUCTION

It is well known that when high-frequency electromagnetic waves are incident on a metal slab the interior of the slab is shielded from the fields by currents established within the skin depth δ. Recent experiments on a number of high-purity metals at low temperatures have shown that long-mean-free-path (λ) conduction electrons moving normal to the surface (ineffective electrons) can transmit small amounts of high-frequency radiation well beyond the skin depth. When an external magnetic field $\vec{H}$ is oriented normal to the surface of a thin slab (or at an angle θ away from normal, $\theta\langle\frac{1}{2}\pi - \delta/\lambda$) these ineffective electrons traveling in well-defined trajectories can cross the sample and in special cases produce a detectable emergent electric field whose phase varies directly with H. Gantmakher and Kaner[1] first observed these weak transmitted fields in tin. The so-called Gantmakher-Kaner (GK) oscillations have since been reported for several metals at radio frequencies[2-7] and recently for potassium,[8] and copper and silver[9] at microwave frequencies.

At radio frequencies the oscillation period is proportional to $m^*\langle v_H\rangle$, the product of the effective mass and the average Fermi velocity parallel to $\vec{H}$. Only electron orbits for which $m^*\langle v_H\rangle$ is extremal contribute to the signal. At microwave frequencies the transmitted signal can be conveniently studied for H both above and below cyclotron resonance and it is sometimes possible to independently determine m^* or $\langle v_H\rangle$.[8,9] In addition signals from orbits for which $m^*\langle v_H\rangle$ is not extremal have also been observed at these higher frequencies.[9]

We report here the results of a microwave transmission experiment in gallium in which many GK oscillation branches arising from different orbits on the Fermi surface (FS) have been observed. The FS of gallium has previously been studied by a variety of experimental techniques some of which are the de Haas–van Alphen (dHvA) effect,[10,11] the radio-frequency size effect,[12,13] Azbel-Kaner cyclotron resonance (AKCR),[14] acoustic cyclotron resonance,[15] magnetoresistance,[16] and oscillatory dc magnetoresistance[17] (the dc analog of the GK oscillations). Much of the data have been explained in terms of the FS model of gallium by Reed[18]; however, the origins of some of the data are still uncertain owing to the complex nature of the FS. In addition, the data of one experiment often appear unrelated to that of another. The identification and correlation of data is especially difficult for experiments which measure differentials of the FS, such as m^* and $m^*\langle v_H\rangle$, since these quantities are most sensitive to small changes in the FS model. This experiment was designed to improve the correlation of data from different experiments by simultaneously measuring $(m^*\langle v_H\rangle)_{\text{extremal}}$ and m^*, which also enables $\langle v_H\rangle$ to be evaluated. Definite independent determinations of both m^* and $(m^*\langle v_H\rangle)_{\text{extremal}}$ was possible for only two branches, however many other GK branches bore sufficiently close resemblance to AKCR extremal-mass branches[14] for comparisons to be made. One GK branch was also identified with a dHvA extremal area branch.

II. BACKGROUND AND THEORY OF GK OSCILLATIONS

Many salient features of the transmitted electric field can be obtained by considering a two-field model in place of the actual complex field distribution inside the metal. The bulk of the electric field is confined to the skin depth and serves to (i) shield the interior of the metal from the external field and (ii) launch ineffective electrons which will carry a small second field into the metal. Ineffective electrons moving through the skin depth receive a small increment to their momentum from the transverse fields there. As they move into the metal along the magnetic field lines, the direction of the increment of momentum rotates with an angular frequency $\omega_c = eH/m^*c$. The nonequilibrium momentum distribution for many such electrons gives rise to a small field inside the metal.

At a depth z inside the metal the field produced by electrons from the same orbit in k space has rotated with respect to the original field direction in the skin depth through an angle $\omega_c z/\langle v_H\rangle$. The angle of the transverse electric vector at z with respect to the instantaneous electric vector in the skin depth is

$$\phi(H) = [(\omega \pm \omega_c)/\langle v_H\rangle]z \ , \tag{1}$$

where ω is the frequency of the applied field and the $\pm$ correspond to the two possible senses of circular polarization. The phase shift of the electric field which emerges at the second surface is also given by this factor,[19] where z is replaced by the sample thickness L. In general both ω_c and $\langle v_H\rangle$ depend on the exact orbit on the FS, so fields produced by electrons having different values of momentum parallel to $\vec{H}$, k_H, will have different phases at the second surface and will tend to cancel. Phillips, Baraff, and Schmidt[9,20] have shown that if $\phi(H)$ is extremal for a certain value of $k_H = k_H'$, i.e.,

$$\frac{\partial\phi(H, k_H)}{\partial k_H} = \frac{\partial}{\partial k_H}\left(\frac{\omega \pm \omega_c}{\langle v_H\rangle}\right)_{k_H = k_H'} L = 0, \tag{2}$$

then electrons from that region of the Fermi surface will be sufficiently in phase to produce a net transmitted electric field.

At radio frequencies, $\omega \ll \omega_c$ for magnetic fields of interest and Eq. (2) reduces to the familiar condition $(m^*\langle v_H\rangle)_{\text{extremal}} = \hbar/2\pi\ (\partial A/\partial k_H)_{\text{extremal}}$ for the observation of GK oscillations, where A is the cross-sectional area of the FS perpendicular to k_H. Where $\partial A/\partial k_H$ is a true extremum, the conduction electrons follow helical trajectories. In addition to signals from electrons on extremal helical trajectories, limiting-point electrons can also yield signals. At the limiting point of the FS, $\partial A/\partial k_H$ is extremal because it is nonzero and terminates here. Since there are only a few electrons in the vicinity of the limiting point, the signal is correspondingly weaker than that of an extremal helical trajectory.[1]

Equation (2) also predicts signals which can only be observed when $\omega \sim \omega_c$. Consider a FS with a constant value of ω_c over a range of k_H values. Equation (2) yields

$$\frac{(\omega \pm \omega_c)}{\langle v_H\rangle^2}\frac{d\langle v_H\rangle}{dk_H} = 0 \tag{3}$$

in this region of constant ω_c. Since $m^*\langle v_H\rangle \alpha\ \partial A/\partial k_H$, Eq. (3) is satisfied by the specific orbit with extremal $\partial A/\partial k_H$, as before. However at $\omega = \omega_c$ all orbits in this region satisfy Eq. (3) and a strong burst of power occurs. For a FS with α-fold symmetry about $\vec{H}$, Eq. (2) becomes[9,20]

$$\frac{\partial}{\partial k_H}\left(\frac{\omega \pm n\omega_c}{\langle v_H\rangle}\right)\Bigg|_{k_H = k_H'} L = 0 \ , \tag{4}$$

where $n = \alpha j \pm 1$, j an integer.[6] Thus, in addition to a strong signal at the cyclotron resonance field $H_c = m^*c\omega/e$, signals are expected at certain harmonics H_c/n. Such bursts of transmitted power have been observed in copper and silver[9,20] and have been termed cyclotron phase resonance.

The arguments leading up to Eq. (2) as the condition for observing a transmitted signal assume that all ineffective electron orbits on the FS can be treated identically. This is not strictly true. Electrons with small values of $\langle v_H\rangle$ may have too small a mean free path to reach the second surface. Also peculiarities in the orbit may allow certain electrons to spend a greater than average time in the skin depth and hence interact more effectively with the exciting field. Baraff and Phillips[9,21] have observed signals in copper and silver arising from such orbits of high "topological effectiveness."

We consider now the calculation of the high-frequency Gantmakher-Kaner mode in a metal slab with specular surface scattering. The mathematical basis of the GK oscillations is the presence of branch points in the wave-vector-dependent conductivity $\sigma(q)$. Gantmakher and Kaner[1] first calculated the long-range electric field mode in a semi-infinite slab which resulted from these branch points. Antoniewicz[22] and Falk, Gerson, and Carolan[23] considered the finite slab case with specular scattering at low frequencies ($H \gg H_c$) and short mean free path ($\lambda < L$). The new aspects discussed here extend their results by calculating the transmitted electric field for arbitrary values of λ and H. These conditions are required to properly describe the field transmitted through a high-purity metal at microwave frequencies. Other conditions of the calculation are: (i) the FS has axial symmetry about $\vec{H}$; (ii) $\vec{H}$ and the direction of the incident circularly polarized electromagnetic wave are normal to the surface; (iii) only contributions to the transmitted electric field from the branch points of $\sigma(q)$ are considered; (iv) the transmitted field is assumed to radiate into free space, not a microwave cavity.

Overhauser and Rodriquez[24] have shown that for a FS with axial symmetry about $\vec{H} \parallel \vec{z}$, the conductivity is given by

$$\sigma_\pm(q) = \frac{ie^2}{(2\pi)^2}\frac{eH}{c}\int_{FS}\frac{dp_z}{\omega_c}\frac{v_\perp^2}{\omega \pm \omega_c + i/\tau - qv_z} \ , \tag{5}$$

where v_z and $v_\perp$ are the electron velocity components parallel and perpendicular to $\vec{H}$, p_z is the electron momentum component parallel to $\vec{H}$, and τ is the momentum scattering time. Antioniewicz[22] and Falk *et al.*[23] have shown that the ratio of transmitted to incident electric field for a specular-

ly reflecting slab of thickness L is given by

$$\frac{E_t^{\pm}}{E_i^{\pm}} \sim \frac{2i\omega}{Lc} \sum_{n=-\infty}^{\infty} \frac{(-1)^n}{(n\pi/L)^2 - (4\pi i\omega/c^2)\sigma_{\pm}(n\pi/L)} . \quad (6)$$

Antoniewicz has evaluated the sum by solving a contour integral. One can show that

$$\frac{E_t^{\pm}}{E_i^{\pm}} \sim \frac{\omega}{Lc} \oint \frac{\csc(\pi z)\, dz}{k_z^2 - (4\pi i\omega/c^2)\sigma_{\pm}(k_z)} - \frac{2i\omega}{Lc} \sum \mathrm{Res}\left(\frac{\pi \csc(\pi z)}{k_z^2 - (4\pi i\omega/c^2)\sigma_{\pm}(k_z)} \right), \quad (7)$$

where $k_z = \pi z/L$ and the integration encloses the entire complex z plane. For gallium at high frequencies, the last term is negligible. It describes the skin-effect fields which have a very short range ($\sim 10^{-5}$ cm). In a noncompensated metal it also predicts the existence of helicon modes.[22,23] The poles also produce the Doppler-shifted cyclotron resonances[23] which at microwave frequencies occur at magnetic fields well above the range of the magnet used in this work.

The contour integral in Eq. (7) will be nonzero if $\sigma(k_z)$ contains a branch point at $z = z'$, in which case there is a contribution to the integral along the branch cut. To show this, let $w = z - z'$ and expand the cosecant term into an infinite series. For z' in the upper half-plane, Eq. (7) becomes

$$\frac{E_t^{\pm}}{E_i^{\pm}} \sim \frac{2\omega}{Lc} \sum_{n=0}^{\infty} e^{(2n+1)iLk_{z'}} \int_{\substack{\text{branch} \\ \text{cut}}} \frac{e^{(2n+1)i\pi w}\, dw}{(\pi/L)^2(w+z')^2 - (4\pi i\omega/c^2)\sigma_{\pm}[(\pi/L)(w+z')]} \quad (8)$$

The integral in Eq. (8) was solved analytically or numerically for a number of FS models characteristic of an extremal helical trajectory or limiting-point resonance. Since the FS of gallium consists of many separate pieces,[18] a two ellipsoid model was also calculated with an appropriate σ for each piece. In this model a large ellipsoid provides the bulk of the conductivity, while a small ellipsoid produces the oscillating signal. All of the models have branch points at $k_{z'} = (\omega \pm \omega_c + i/\tau)/v_z$ and yield a transmitted field of the form

$$\frac{E_t^{\pm}}{E_i^{\pm}} \sim \frac{v_z}{c} \sum_{n=0}^{\infty} T_{2n+1}(\omega \pm \omega_c)\, e^{-(2n+1)L/\lambda} \times \exp[i(\omega \pm \omega_c)(L/v_z)(2n+1) + i\alpha_{2n+1}(\omega \pm \omega_c)]. \quad (9)$$

The essential features of the specular scattering case are (i) $E_t^{\pm}/E_i^{\pm}$ contains a fundamental and odd harmonics.[25] The presence of harmonics is the direct consequence of specular scattering. An electron scattered at the surface has its momentum normal to the surface reversed while the transverse component is preserved. For long λ electrons, the sample appears to have a thickness $L' = (2n+1)L$ for the $(2n+1)$ harmonic; (ii) the n-dependence of the amplitude is closely given by $T_{2n+1} = (2n+1)^{-P}$, except in the immediate vicinity of cyclotron resonance. For extremal helical trajectories $p = \frac{3}{2}$, while for limiting points $p = 2$[26]; (iii) the fundamental and harmonics all have an essentially symmetric amplitude dip at cyclotron resonance ($-$ component). Above resonance, the amplitude continues to increase with increasing H until $H \gg H_c$, where a rapid decrease begins; (iv) for the single ellipsoid and extremal helical trajectory cases the phase angles α_{2n+1} are relatively small except near resonance for all harmonics. Addition of the second ellipsoid further reduces α_{2n+1} to about 0.2 rad when the magnetic field is $\frac{1}{2}H_c$ away from resonance.

This type of signal is in contrast to that expected when the surface scattering is diffuse. Baraff[27] has calculated the transmitted field for a spherical FS. The diffuse case has an amplitude peak at cyclotron resonance and the phase angle changes from $-\frac{1}{2}\pi$ below resonance to $+\frac{1}{2}\pi$ above resonance. No harmonics are present since the diffuse scattering causes the electrons to loose all phase memory. Experiments on potassium have verified the amplitude peak[8] and phase shift[7] of this theory.

The relative amplitudes of the specular and diffuse signals depends on magnetic field strength and scattering time τ but the diffuse signal can be two or three orders of magnitude greater, especially at resonance.

None of these calculations uses a FS as complex as that of gallium. A calculation of the transmitted field using the known FS of gallium would be extremely difficult. However at least one GK branch observed here is known to originate on a small, nearly ellipsoidal FS piece[28] and for this case the two ellipsoid model may not be too unrealistic. A more realistic model might be to treat the electrons on the large ellipsoid as being scattered diffusely while those on the small ellipsoid are scattered specularly.

III. EXPERIMENTAL PROCEDURE

The measurements were made using a closed-loop transmission apparatus in which the sample forms a common wall between two microwave cavities. Similar schemes have been used to study conduction-electron spin resonance in metals.[29,30]

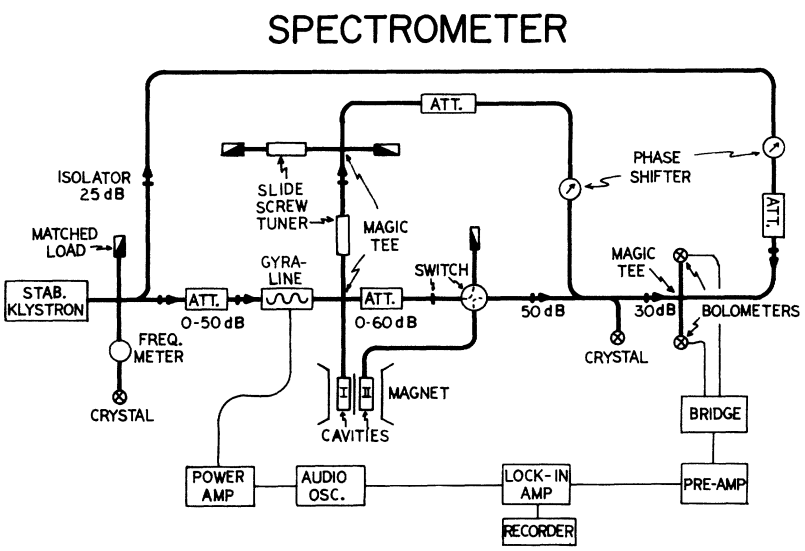

FIG. 1. Schematic diagram of the microwave transmission spectrometer. Heavy lines represent waveguide.

A diagram of the apparatus is shown in Fig. 1. Microwave power, amplitude modulated at 100 Hz by a Gyraline, is incident on the transmitter cavity I. Cavity I is tunable so that both cavities can be brought to the same resonance frequency of 9.23 GHz. A rotary switch allows reflected power from cavity I, as well as transmitted power from the receiver cavity II, to be detected by the bolometers. The isolation of the rotary switch is only 60 dB so the reflected power from cavity I was attenuated by an additional 60 dB when the transmitted signal was being observed. At the bolometers the transmitted field is beat against a reference field whose phase can be varied through 360°. The resulting signal is detected and recorded in the standard way.

To avoid thermal straining or cracking of the thin gallium samples they were suspended by tabs between the two cavities until the operating temperature of 1.3 °K was obtained. The cavities were then clamped together. Usual methods for reducing leakage between the cavities, such as conducting paint and indium O-rings, could not be used because of this clamping arrangement. The leakage power was reduced by introducing into the signal arm a second signal with the same magnitude but opposite phase from the leakage signal. Using this scheme the unbalanced leakage power could be reduced to $\sim 5\times10^{-17}$ W for an incident power of 10^{-1} W. This residual leakage power is almost independent of H and generally causes no operating difficulties.[31] Over-all spectrometer sensitivity is better than 10^{-19} W for a 1-Hz bandwidth.

Samples were grown from 99.9999% pure gallium in Plexiglass molds. Each sample had one of the crystallographic axes (given by the capital letter in the name) within 1° of the sample normal $\vec{n}$. Surface areas of the samples were made large, typically ~ 1 in.^{2}, to help reduce microwave leakage. The sample thickness was determined by measuring the surface area and mass of each sample and using the room-temperature density of 5.907 g/cm^3. The following thermal contractions[32] were used to get the 1.3 °K thicknesses for a-, b-, and c-axis samples, respectively: $\Delta L/L = 2.41\times10^{-3}$; 6.99×10^{-3}; 4.11×10^{-3}. Table I lists the samples and thicknesses.

The samples were oriented between the cavities so that the microwave current, $\vec{j}$, was along a crystal axis. The transmitted GK signal has been calculated only for the case $\vec{H} \parallel \vec{n}$, however data were taken at regular intervals for $\vec{H}$ in the plane of $\vec{n}$ and $\vec{j}$. The principal effect of rotating $\vec{H}$ an angle θ away from $\vec{n}$ is to change the effective thickness of the sample to $L/\cos\theta$. The precise orbit responsible for a set of oscillations also changes with θ and this sometimes effects the line shape.

IV. EXPERIMENTAL RESULTS

A. General Features

Sample-size-dependent oscillations were observed in each of the principal planes of gallium.

TABLE I. Samples and thicknesses.

Sample	Thickness (mm) 300 °K	1.3 °K
B-I	0.0707	0.0702 ± 0.0010
B-II	0.109	0.108 ± 0.003
B-III	0.128	0.127 ± 0.002
B-IV	0.185	0.184 ± 0.002
B-V	0.243	0.241 ± 0.002
B-VI	0.509	0.505 ± 0.005
A-I	0.126	0.126 ± 0.001
C-I	0.191	0.190 ± 0.002

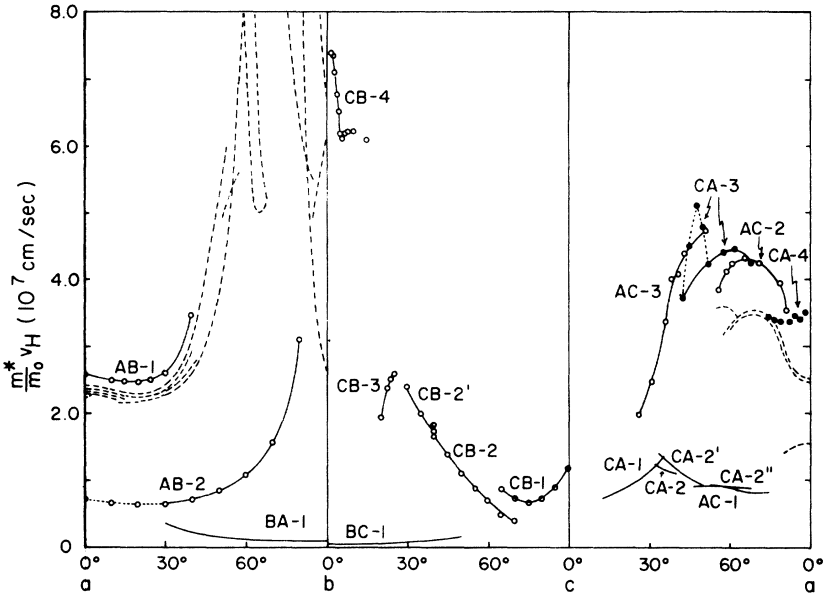

FIG. 2. Size-effect data in the three principal planes of gallium. Dashed lines are from the dc Sondheimer oscillations (Ref. 17). Dotted lines indicate uncertainty in the period, see text.

The measurable quantities L and oscillation period ΔH are related to orbit parameters by the following expressions:

$$\frac{\Delta HL}{\cos\theta} = \frac{\hbar c}{e}\left(\frac{\partial A}{\partial k}\right) = \frac{2\pi c}{e} m^*\langle v_H\rangle . \qquad (10)$$

Figure 2 shows the size-effect data obtained in this experiment. The branches are designated by two letters; the first gives the sample normal and the second the direction of the microwave current. The data are plotted for convenience as the quantity $(m^*/m_0)\langle v_H\rangle$. The dashed curves are the data obtained by Munarin, Marcus, and Bloomfield[17] from the Sondheimer oscillations in the dc magnetoresistance of gallium. These oscillations are known to come from orbits where $\partial A/\partial k$ is extremal. Comparison of the two sets of data[33] shows only one branch, AB-1, in approximate agreement with a dc branch. A possible explanation for the disparity between the two sets of data is that the two experiments may have greatly differing sensitivities depending on the magnitude of ΔH. The strongest oscillations at microwave frequencies were those with small ΔH, and presumably small m^*. Moore,[14] who measured the AKCR in gallium, also noted that the small-mass branches were the most intense. The dc experiment was probably less sensitive to rapid oscillations than to slow oscillations. Branch BC-1, which is extremely intense at microwave frequencies, would have a period ΔH less than the width of the field modulation used by Munarin *et al.* and is unlikely to have been observed in their thicker samples.

Another possibility for the differences between the two sets of data is that the microwave branches are not due to orbits of extremal $\partial A/\partial k$ but may arise from one of the other mechanisms mentioned in Sec. II. Branch BA-1, in fact, is known to be due to cyclotron phase resonance. Baraff and Phillips[9,21] have pointed out, however, that GK oscillations arising from orbits with maximum topological effectiveness will only occur if $\omega > \omega_c$. Gallium is characterized by many small effective mass branches[14] so most resonant fields are less than 2 kOe at the frequency of this experiment. The majority of the observed branches have oscillations continuing well above this field with many still increasing in magnitude at 10 kOe, the highest attainable field for these experiments. It is thus unlikely that the "topological effectiveness" mechanism is operative in these cases.

A surprising result of the experiment is that in no case is the expected symmetric peak or dip at cyclotron resonance observed in the GK oscillations. Several branches show an amplitude increase with H starting at low fields. These cases may actually be characteristic of oscillations produced by specularly scattered electrons (i.e., symmetric dip at H_c) with small effective mass. The signal-to-noise ratio is too poor at low fields to observe oscillations increasing in amplitude as H is lowered below H_c. Values of m^* were obtained for two branches which have anomalies at H_c. Branch BA-1 is characteristic of cyclotron phase resonance while BC-1 contains an unexplained asymmetric amplitude anomaly at H_c.

Several of the size-effect branches show a great similarity to AKCR effective-mass branches[14] in field dependence, angular range, and polarization effects and it is likely that nearby orbits on the same piece of FS are responsible for the two effects.

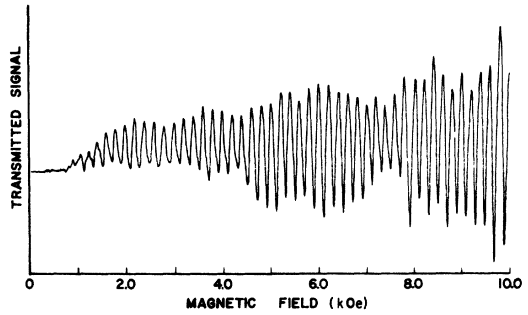

FIG. 3. Signal transmitted through sample C-I, $\vec{j} \| a$. $\vec{H}$ makes an angle of 30° with the c axis in the ca plane. A beat period of ~1 kOe is observed due to interference between branches CA-1 and CA-2.

B. Specific Features of the Data

The size-effect oscillations observed in gallium at microwave frequencies were of several types. The particular type observed depended in part on sample thickness and the strength and degree of tilt of the magnetic field, as well as the properties of the individual orbits.

1. Small Period Oscillations of Ineffective Electrons

This type of oscillation showed the greatest resemblance to the calculated GK oscillations. Electrons which have no portion of their orbit moving parallel to the sample surface will absorb and reradiate electrical energy uniformly along their helical trajectory producing a sinusoidal signal. Most of the signals observed for $\vec{H}$ near the sample normal—BC-1, CA-1, CA-2, and CA-2′—are of this type. The signals are generally weak or unobservable at low magnetic fields (below the cyclotron resonant field H_c) and increase gradually with increasing field strength. The oscillations of BC-1 differ in this latter respect and will be discussed separately in a later section. The observation of GK oscillations only above resonance is in marked contrast to the oscillation from electrons of high topological effectiveness observed in copper and silver[9] which occurred only below H_c.

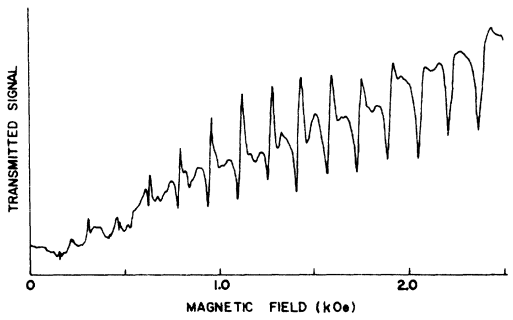

FIG. 4. Sharp spikes of branch AB-2 seen in the signal transmitted through sample A-I, $\vec{j} \| b$. $\vec{H}$ makes an angle of 70° with the a axis in the ab plane.

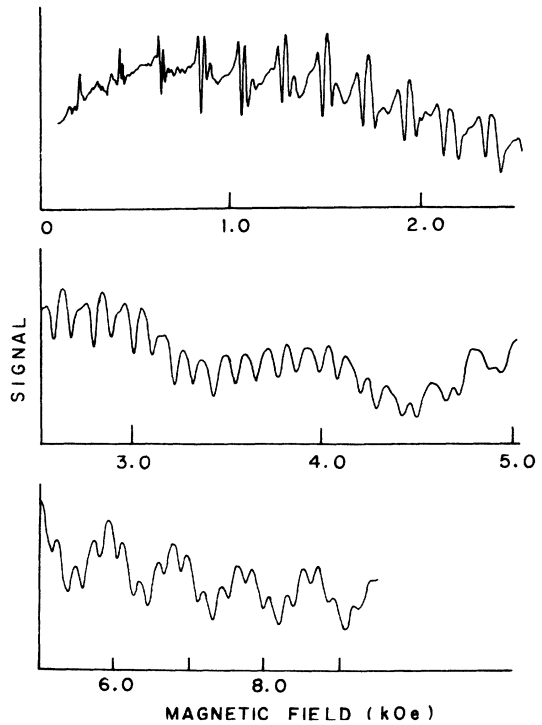

FIG. 5. Signal transmitted through sample A-I, $\vec{j} \| c$. $\vec{H}$ makes an angle of 55° with the c axis in the ca plane. At low fields (top trace) the sharp double spikes of AC-1 are seen. They broaden and in a certain field range (middle trace) give a sinusoidal signal with $\frac{1}{2}$ the average period. At high fields (bottom trace) they have the average period and are superimposed on the broad AC-2 oscillations. Note the change in scale.

Figure 3 shows the signal transmitted through sample C-I with $\vec{H}$ 30° from the c axis and $\vec{j} \| a$. A beat period of ~1 kOe is observed which is due to interference between branches CA-1 and CA-2. Branch CA-1 and Moore's AKCR mass branch G have a similar angular dependence and are believed to arise from the same or neighboring orbits on the FS. This would make the resonant field in Fig. 3, 300–400 Oe. The amplitude dependence of the oscillations above resonance is in qualitative agreement with the various calculations assuming pure specular surface scattering. Under the conditions of Fig. 3 oscillations are not observed until $H > 2H_c$. One would not expect to observe oscillations in the field range $0 \leq H \leq 2H_c$ since all FS models based on pure specular surface scattering predict a symmetric amplitude dip at resonance.

2. Oscillations of Effective Electrons

Electrons which have a portion of their orbit moving parallel to the surface will preferentially

absorb and reradiate electrical energy during these effective segments of their trajectory.[6,34] The signal consists of sharp spikes at field values of $n\Delta H$, $n = 1, 2, 3, \ldots$, where ΔH is the GK period. The signal passes through cyclotron resonance with no noticeable change in amplitude or phase. This type of signal generally occurs for H far from the sample normal, as with branches AB-2, CA-2$''$, and AC-1. Branch AB-1 produced periodic spikes even for $\vec{H} \parallel \vec{n}$. Large periodic current splashes of this type for $\vec{H}$ normal have previously been observed in copper at radio frequencies.[6] Between the sharp spikes of AB-1, weak sinusoidal signals appear which are characteristic of the third and sixth harmonics of the GK period. These signals interfer with those of AB-2 and make the determination of the latter's period uncertain near the a axis (dotted curve in Fig. 2).

Figure 4 shows oscillations from branch AB-2 characteristic of the type of signals produced by electrons with an effective trajectory segment. The spikes generally increase in amplitude and broaden with increasing magnetic field, eventually becoming a sinusoidal signal of the same period. Branch AC-1, Fig. 5, shows a definite double spike as if two sets of oscillations of nearly equal period are superimposed. From 3 to 4 kOe, the spikes have broadened and are out of phase, producing a nearly sinusoidal variation of half the average period. At higher fields the oscillations are again in phase and the average period appears superimposed on the large period oscillations of branch AC-2. At certain angles the double spikes are observed to

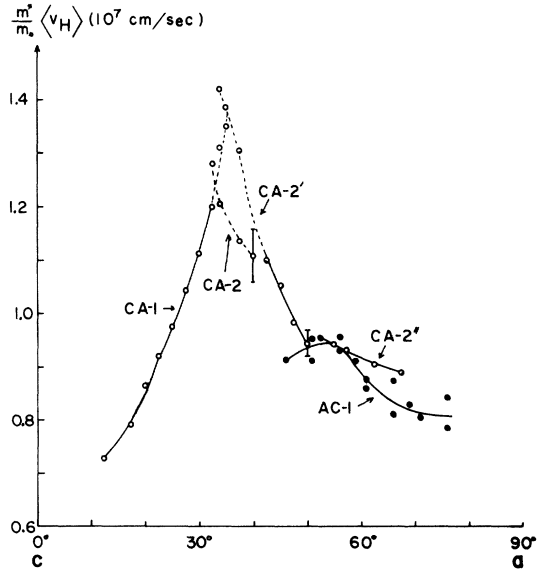

FIG. 6. Small-period size-effect data in the ac plane. Dotted lines indicate an uncertain region where three branches cross.

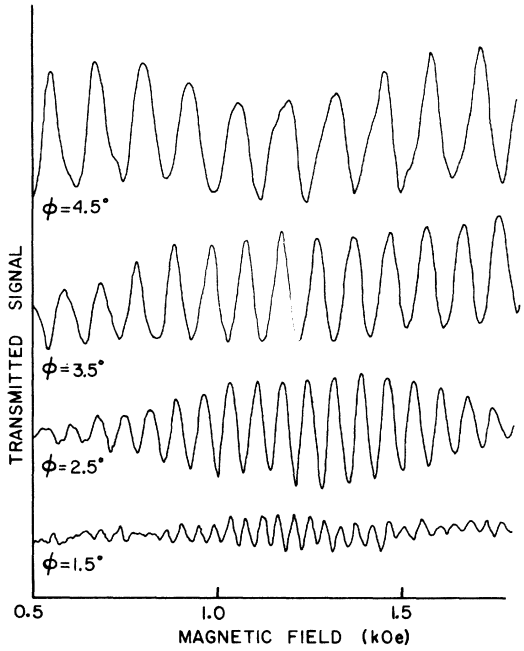

FIG. 7. Transmitted signal for branch CA-4 for small tilt angles, ϕ, of $\vec{H}$ out of the sample plane.

coalesce into a single broadened spike providing only the average period (see Fig. 6). Unlike two sinusoidal signals which produce a beating pattern, it is difficult to distinguish two nearly identical sets of periodic spikes from a single set with side structure which broadens with field. The belief that two sets are present here is strengthened by the nearly parallel branches CA-2, CA-2$'$, and CA-2$''$ in the $\vec{j} \parallel \hat{a}$ polarization case and the close resemblance of the size effect branches in the ac plane (Fig. 6) to Moore's mass branches G and the parallel set F and F'. It is likely that the extremal mass orbit and the corresponding size effect orbit are nearby orbits on the same piece of FS.

3. *Limiting Point Resonances at Large Angles*

Two sets of oscillations, CA-4 and CB-4, were observed for $\vec{H}$ only a few degrees out of the sample plane. At these angles, the effective thickness of the sample, $L/\cos\theta$, approaches 1 cm and only electrons with the longest mean free paths can cross the sample without scattering. The oscilla-

TABLE II. $(m^*/m_0)\langle v_H\rangle$ for branches CA-4 and CB-4 and comparison with the calculated values for the 8e ellipsoid (in units of 10^7 cm/sec).

	Experiment	Theory	
		Reed	dHvA
$\vec{H} \parallel \hat{a}$	3.46 ± 0.08	3.02	3.98
$\vec{H} \parallel \hat{b}$	7.4 ± 0.2	8.77	7.06

tions are thus thought to arise from orbits at or very near a limiting point. These electrons are also the ones most excited by the field in the skin depth, since $\vec{H}$ is nearly parallel to $\vec{j}$. Figure 7 shows traces of CA-4 for angles of 1.5° to 4.5° out of the sample plane. The qualitative behavior of CB-4 is the same as that of CA-4. CB-4 was observable as far as 19.7° away from the b axis and CA-4 as far as 13.0° from the a axis. Gantmakher and Kaner[34] and others[4] have observed similar oscillations at radio frequencies for $\vec{H}$ just out of the sample plane. The rf experiments produced periodic spikes characteristic of orbits with effective segments. Only a sinusoidal variation was observed in the present case. However, no signals were observed at low fields where the sharp nature of the spikes should be most noticeable.

Table II gives the values of $(m^*/m_0)\langle v_H\rangle$ along the a and b axes. For comparison, two calculated limiting point values for each direction are given for the eighth band ellipsoid centered at L. The first value is calculated using extremal area of the ellipsoid from Reed's pseudopotential calculation of gallium.[18] The second value uses the dHvA extremal areas obtained by Goldstein and Foner[10] and Condon[11] along the a and b axes and Reed's calculated c-axis area (for which no dHvA data for this piece are available). The calculations assume a perfect ellipsoidal FS, however, the true surface undoubtedly differs somewhat from this idealization. An ellipsoid with its major axis along k_c also predicts a rapid decrease in $(m^*/m_0)\langle v_H\rangle$ as H is rotated towards the c axis. Branch BC-4 is in good qualitative agreement with this.

The decrease in amplitude of the signals as $\vec{H}$ approaches the sample plane (see Fig. 7) is due to two factors. First, there is an exponential decrease in amplitude with effective thickness given by $\exp(-L/\lambda\cos\theta)$. Second, the sample surface area which can radiate power also decreases with increasing θ due to the finite thickness and area of the sample.[34] This latter term is complicated by the possibility of small-leakage fields at the edges of the sample. The variation in amplitude of CB-4 near the b axis yields $\lambda \sim 4.3$ mm at 1.3 °K.

4. *High-Field Large-Period Oscillations*

One group of oscillations in the ca plane, AC-2, AC-3, and CA-3, are characterized by large periods of order $\Delta H \sim 1$ kOe and appreciable strength only at high fields, generally above 4 or 5 kOe. If signals are weak in the vicinity of cyclotron resonance and are only observable at higher fields, then the only difference between this group of oscillations and the small-period ineffective-electron oscillations is a larger value of m^* in this case. Because of the large periods only a few oscillations are observed below 10 kOe. Figure 5 shows AC-2 as a broad background variation for the rapid oscillations of AC-1. The oscillations of the three branches, AC-2, AC-3, and CA-3, are sinusoidal with the exception of AC-3, which becomes a periodic spike as $\vec{H}$ approaches the c axis.

Approximately 40° to 50° from the a axis, branch CA-3 undergoes a rapid increase in period and then returns to its expected extrapolated value (see Fig. 2). It is not clear whether or not this departure represents another branch crossing CA-3. The limited number of oscillations which can be observed does not allow beating patterns to be resolved.

There is a similar behavior for branches AC-2 and AC-3 using the $\vec{j} \parallel c$ polarization. As $\vec{H}$ is rotated towards the c axis, the signal from AC-2 suddenly fades and AC-3 appears a few degrees away with a larger period.

The qualitative similarity between the large period branches for the two polarizations suggests that nearly the same orbits are being excited in both cases.

5. *Oscillations in the cb Plane, $\vec{j} \parallel \hat{b}$ Axis*

The oscillations observed under these conditions are characterized as extremely weak with periods that are nonconstant. The oscillation period often changes a few percent after several cycles at a constant period. This behavior is not the same as that observed in copper by Perrin *et al.*[6] in which different harmonics of the fundamental period were observed for different field ranges. In the present case, a period observed at low fields often reappears at a higher field. At isolated angles the signal is quite intense and extends over a large-field range. The data given in Fig. 2 for these branches represent the most intense and continuous oscillations observable in this plane.

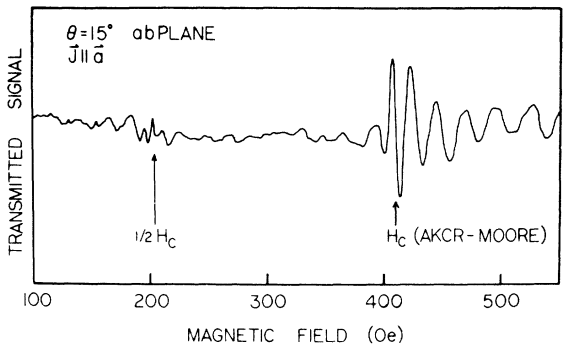

FIG. 8. Oscillations of branch BA-1 transmitted through sample B-II. This signal is characteristic of cyclotron phase resonance. H_c is the cyclotron resonance field observed by Moore (Ref. 14) for mass branch L.

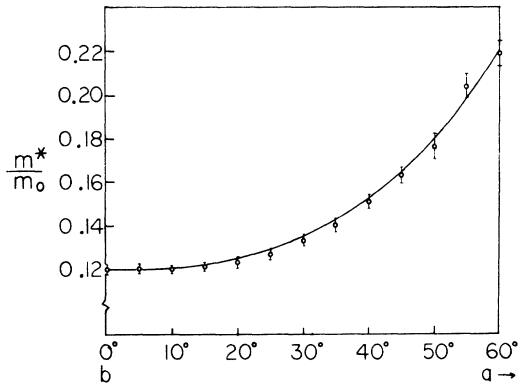

FIG. 9. Effective mass obtained from branch BA-1 in the ba plane. The solid curve is the value observed by Moore (Ref. 14) for mass branch L.

6. *Cyclotron Phase Resonance in Thin Samples*

The b-normal samples with $\vec{j} \parallel \hat{a}$ exhibited no size-effect branches except for the thinnest sample used, B-II. (Sample B-I was accidently destroyed before the $\vec{j} \parallel a$ polarization case could be studied.) These oscillations, BA-1 (see Fig. 8), are characteristic of cyclotron phase resonance with sharp bursts of power at cyclotron resonance H_c. There is also a noticeable burst of power at half the resonant field but not at any other harmonics H_c/n. Equation (4) allows a value of $n=2$ since $\alpha=1$ for $\vec{H}$ in the ab plane. m^* was determined by taking the resonant field as twice the value of the peak oscillation near $\frac{1}{2}H_c$. Phase effects are less sensitive here since the oscillations are more rapid than near H_c. The value of m^* agrees closely with Moore's AKCR mass branch L over a 60° range as shown in Fig. 9. The periodic oscillations of BA-1 continue for at least 10 cycles above resonance at most angles enabling $(m^*/m_0)\langle v_H\rangle$ to be obtained.

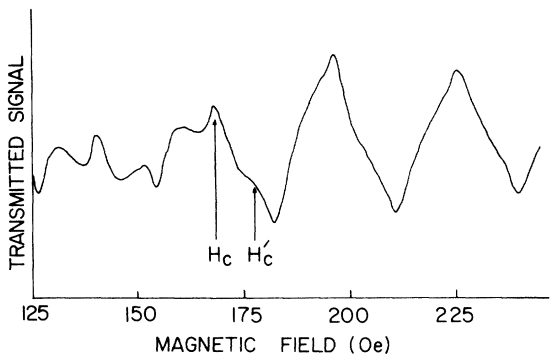

FIG. 10. BC-1 oscillations near cyclotron resonance in sample B-I, $\vec{H}$ normal. H_c is the cyclotron resonance field for Moore's mass branch C (Ref. 14) and H_c' is the resonance field inferred from the dHvA data of Goldstein and Foner (Ref. 10).

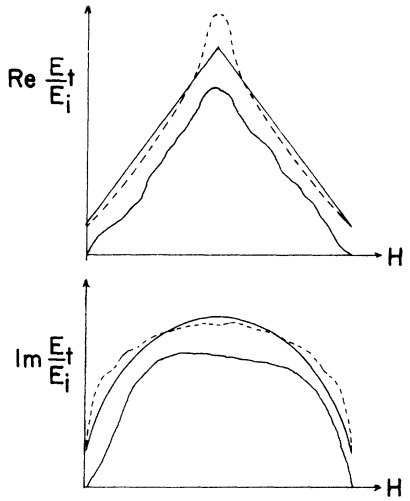

FIG. 11. Top trace: Experimental trace of the real component of the field transmitted through Sample B-II. The solid curve is the theoretical line shape for $p=2$; the dashed curve is for $p=\frac{3}{2}$. Bottom trace: Experimental curve (imaginary component) after a 90° reference phase change. The solid curve is the theoretical line shape for $p=2$; the dashed curve is for $p=\frac{3}{2}$. In both sets of curves the theoretical curves are displaced upward for clarity. There is actually a $\frac{1}{4}\Delta H$ shift in peak field positions between the two sets which is not indicated.

C. BC-1 Oscillations

The line shape of the BC-1 oscillations was studied extensively as a function of magnetic field strength, sample thickness, and spectrometer phase. The line shape strongly supports the theory that the electrons responsible for these oscillations are scattering specularly, as has previously been reported.[28] Figure 10 shows a dramatic change in line shape of BC-1 near 170 Oe. The field value for the onset of the more normally shaped GK oscillations is independent of sample thickness, decreases by 5% with a 5% reduction in microwave frequency, and increases as $\vec{H}$ is rotated away from the sample normal. The onset is in excellent agreement with the cyclotron resonance field for Moore's mass branch C over a 50° range in the bc plane.[28] Both branches are believed to originate from a small nearly ellipsoidal five-band-hole FS piece in Reed's model. The identification is made via dHvA extremal area and effective mass data.[10,11] For $\vec{H} \parallel \hat{b}$, AKCR yields $m^* = 0.0513 m_0$ while dHvA data yield $m^* = .054 m_0$ for this FS piece.

The line shapes of the GK oscillations above resonance show considerable harmonic content due to the multiple reflections. Equation (9) predicts various signal line shapes depending on the spectrometer phase. Neglecting the phase angle α_{2n+1}, which is small except near resonance, the real part of the signal yields

$$\mathrm{Re}\frac{E_t^{\pm}}{E_i^{\pm}} \propto \sum_{n=0}^{\infty}(2n+1)^{-P}\exp\left(-\frac{(2n+1)L}{\lambda}\right) \times \cos\left(\frac{(\omega \pm \omega_c)(2n+1)L}{\langle v_H\rangle}\right), \quad (11)$$

where the field dependence of the amplitude has been left out. To obtain the imaginary signal, sines replace cosines in the infinite series. For the thinnest samples used, the exponential factor is negligible for the first several harmonics. Figure 11 shows the calculated real and imaginary signals for infinite λ for both the limiting point ($p=2$) and the extremal helical trajectory case ($p=\frac{3}{2}$). Below each set are the experimental curves above resonance obtained with spectrometer phases set 90° apart. One cannot distinguish from the data which of the two cases apply. Fourier analysis of the line shape gives $p \sim 1.7 \pm 0.2$ in the long λ limit at $\omega_c = 1.25\omega$ for sample B-I. As expected the thicker samples show less harmonic content since the exponential term in Eq. (11) is larger.

As the field is increased far above resonance, the relative strengths of the harmonics compared to the fundamental decrease (even in the thinnest samples) due to dephasing effects. When the faces of the sample are not perfectly parallel but have thickness variations of δL then this produces a phase difference of $\delta\phi_n^{\pm} = [(\omega \pm \omega_c)\delta L/\langle v_H\rangle](2n+1)$ between electrons crossing a thickness L and those crossing a thickness $L+\delta L$. When this dephasing effect becomes large enough ($\delta\phi_n^{\pm} \to \pi$) for a particular harmonic, its amplitude will approach zero. All the resonant components have $\delta\phi_n^{-}=0$ at $\omega=\omega_c$ but as the field moves away from H_c the harmonics will dephase faster than the fundamental. This dephasing effect is clearly evident in Fig. 12, where the higher harmonics are largely washed out by 800 Oe. Such a dephasing effect can be accounted for by sample thickness variations of only $\sim\frac{1}{2}\%$.

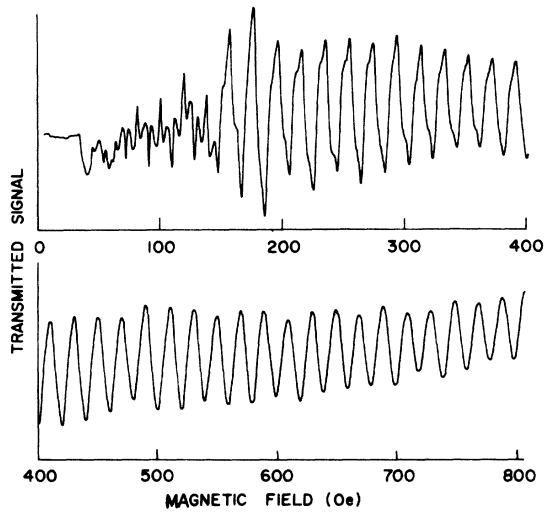

FIG. 12. BC-1 oscillations in sample B-II, field normal. Dephasing effects account for the decrease in harmonic content above resonance.

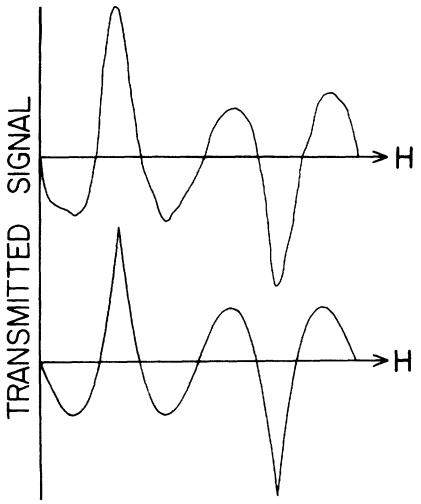

FIG. 13. Top trace: BC-1 oscillations in sample B-I below resonance, field normal. Bottom trace: Calculated curve for a triangle wave ($p=2$) minus the fundamental.

Below resonance the signal line shape of BC-1 is quite different, although the period is the same as above resonance except for a small decrease in ΔH below 100 Oe. Fourier analysis of the signal shows that in going below H_c the amplitude of the fundamental decreases by a factor of 25 while the higher harmonics are essentially unchanged. Figure 13 shows the experimental trace for sample B-I resonance compared with the triangular curve ($p=2$) minus the fundamental. This decrease in the fundamental amplitude occurs very rapidly, within one GK period near cyclotron resonance.

Neither of the simple theories, specular or diffuse, predicts an asymmetric signal amplitude about cyclotron resonance. However, experimental effects might account for the anomaly. Since the microwave cavity produces linearly polarized fields at the first surface, both the + and − circularly polarized components are present in the transmitted field. One always detects the larger-polarization component for $\omega_c \gg \omega$. However, at low fields both components have comparable amplitudes and can interfere. The phases and amplitudes predicted by the current theory do not have the right values to produce low-field cancellation although a more realistic calculation (e.g., considering the effects of the cavities) might alter them enough to do so.

This same interference effect should also apply to the harmonics and this suggests that they should have the same amplitude anomaly as the fundamental. However, the dephasing effects for the + po-

TABLE III. Size-effect data for $\vec{H} \| \hat{b}$.

Branch	$(m^*/m_0)\langle v_H \rangle$ (10^7 cm/sec)	m^*/m_0	$\langle v_H \rangle$ (10^7 cm/sec)
BA-1	0.097 ± 0.005	0.120 ± 0.002	0.81 ± 0.05
BC-1	0.0578 ± 0.0005	0.0500 ± 0.0015	1.16 ± 0.05

larization harmonics can be very large at low fields ($\delta\phi^+ = 3\delta\phi^-$ at $\omega_c = \frac{1}{2}\omega$) so that their amplitudes may actually be much smaller than the – components in this field range and will not interfer strongly.

A second, less satisfactory, explanation considers the effect of a few electrons which scatter diffusely producing a signal which interferes with the specular signal. The diffuse signal exhibits a π phase shift in going through resonance while the specular signal has only a small phase shift. This process only effects the fundamental and is very abrupt at resonance, in agreement with experimental observations. Unfortunately, the amplitudes of the two signals must be nearly the same over a large field range ($\omega_c \sim 0$ to 2ω) to produce the proper interference. This is in such poor agreement with the theoretical amplitudes that this explanation of the anomaly does not seem very promising.

D. Fermi Velocities $\langle v_H \rangle$

Two branches, BA-1 and BC-1, were characterized by anomalies at cyclotron resonance, allowing m^* and $\langle v_H \rangle$ to be determined. The data for these two branches for $\vec{H} \| b$ are summarized in Table III. For both cases, the value of $\langle v_H \rangle$ increases as $\vec{H}$ is rotated away from the b axis, while on the average for the entire FS, b is the high-velocity (low-resistivity) axis. This difference strengthens the supposition that the individual FS pieces responsible for these two sets of oscillations are small with high curvature along k_b, in contrast with the larger pieces for which k_b is the low-curvature axis.[13]

The small-period oscillations in the ac plane show a great resemblance to three AKCR extremal mass branches with the correspondence given in Table IV. The validity of combining the results of the two experiments to obtain $\langle v_H \rangle$ is questionable since the value of m^* may vary considerably between the extremal mass orbit and the nearby extremal $m^*\langle v_H \rangle$ orbit. However this is not the case for branches BA-1 and BC-1 which yield mass values within 2% of Moore's mass branches L and C, respectively, for $\vec{H} \| b$. Combining the data from the branches given in Table IV yields values of $\langle v_H \rangle$ ranging from 8 to 12×10^7 cm/sec. Doppler shifted acoustic cyclotron resonance measurements[15] and heat pulse-time-of-flight measurements[35] for the same direction in gallium have yielded Fermi velocities considerably smaller than those values. To explain the discrepancy, it should be noted that heat-pulse measurements tend to yield only an average of Fermi velocities in a particular direction. If a relatively small number of high-velocity electrons are producing the size-effect oscillations they may be unobservable in a heat-pulse measurement. The acoustic-cyclotron-resonance experiment may also be less sensitive to such a small number of high velocity electrons than is a microwave transmission experiment where the electrons must cross the sample.

V. SUMMARY

Several size-effect branches have been observed in gallium at microwave frequencies. Most of these are believed to be true GK oscillations corresponding to orbits of extremal $\partial A/\partial k$ rather than orbits of maximum topological effectiveness. Several sets of oscillations arising from ineffective electrons have an increase in amplitude above cyclotron resonance, in qualitative agreement with the theory based on specular surface scattering.

One set of ineffective electron oscillations, BC-1, contains the odd harmonics which are predicted for electrons undergoing specular scattering and having $\lambda \gg L$. This branch has an anomalous amplitude behavior at cyclotron resonance for which no adequate explanation is presently available. The effective mass of this branch is in excellent agreement with Moore's AKCR mass branch C.

Oscillations from electrons with effective segments in their trajectories were also observed, even for $\vec{H} \| \hat{n}$. The signal of periodic spikes extends through cyclotron resonance with no observable change, except for a gradual broadening as H is increased.

Two branches of limiting point electrons were

TABLE IV. Correspondence between size-effect branches in the *ac* plane and AKCR extremal-mass branches of Moore (Ref. 14).

Size-effect branch	AKCR mass branch
CA-1	G
CA-2	F'
CA-2′	F
CA-2″	F or F'
AC-1	F or F'

observed for $\vec{H}$ just out of the sample plane. The values of $(m^*/m_0)\langle v_H\rangle$ for these two branches are in reasonable agreement with that expected along the a and b axes for the large 8e ellipsoid in Reed's FS model.

One branch, AB-1, was observed in the thinnest b-normal sample which was characteristic of cyclotron phase resonance. Amplitude peaks occured at H_c and $\frac{1}{2}H_c$ giving a value of m^* which is in excellent agreement with Moore's AKCR mass branch L.

The observation of GK oscillations at microwave frequencies offers an advantage over radio frequencies in allowing the oscillations to be studied on both sides of cyclotron resonance with the possible determination of m^* as well as $(m^*\langle v_H\rangle)_{\text{extremal}}$. This is one of the few methods of measuring Fermi velocities at specific spots on the FS with a single experiment.

The apparent sensitivity of this experiment to FS pieces with small values of m^* has enabled new size-effect branches to be determined. Together with the dc data of Munarin *et al.*,[17] a more complete mapping of $(\partial A/\partial k)_{\text{extremal}}$ is available for gallium.

Finally, correlations have been made between several size-effect branches and AKCR extremal-mass branches. This should help in the eventual identification of these branches with specific electron orbits which will lead to refinements in the present model of the FS of gallium.

ACKNOWLEDGMENTS

I would like to express my appreciation to Professor T. G. Castner for his guidance and encouragement during the course of this research. I would also like to thank Muhlenberg College for financial support during the writing of this manuscript.

---

*Work supported by the U. S. Atomic Energy Commission.

†Paper based in part upon a dissertation submitted in partial fulfillment of the requirements for the degree of Doctor of Philosophy at the University of Rochester.

‡Present address: Physics Department, Muhlenberg College, Allentown, Pa. 18104.

[1]V. F. Gantmakher and E. A. Kaner, Zh. Eksp. Teor. Fiz. **48,** 1572 (1965) [Sov. Phys.-JETP **21,** 1053 (1965)].

[2]P. R. Antoniewicz, L. T. Wood, and J. D. Gavenda, Phys. Rev. Lett. **21,** 998 (1968).

[3]L. T. Wood and J. D. Gavenda, Phys. Rev. B **2,** 1492 (1970).

[4]V. P. Naberezhnykh and A. A. Maryakhin, Phys. Status Solidi **20,** 737 (1967).

[5]S. Foner and E. J. McNiff, Jr., Rev. Sci. Instrum. **38,** 931 (1967).

[6]B. Perrin, G. Weisbuch, and A. Libchaber, Phys. Rev. B **1,** 1501 (1970).

[7]A. Libchaber, G. Adams, and C. C. Grimes, Phys. Rev. B **1,** 361 (1970).

[8]S. Schultz, in *Proceedings of Colloque Ampere XV, Grenoble , 1968* (North-Holland, Amsterdam, 1969).

[9]T. G. Phillips, G. A. Baraff, and P. H. Schmidt, Phys. Rev. B **5,** 1283 (1972).

[10]A. Goldstein and S. Foner, Phys. Rev. **146,** 442 (1966).

[11]J. H. Condon, experimental results are reported by W. A. Reed, Ref. 18.

[12]A. Fukumoto and M. W. P. Strandberg, Phys. Rev. **155,** 685 (1967).

[13]P. H. Haberland, J. F. Cochran, and C. A. Shiffman, Phys. Rev. **184,** 655 (1969).

[14]T. W. Moore, Phys. Rev. **165,** 864 (1968).

[15]J. A. Munarin, Phys. Rev. **172,** 737 (1968).

[16]W. A. Reed and J. A. Marcus, Phys. Rev. **126,** 1298 (1962); J. R. Cook and W. R. Datars, Phys. Rev. B **1,** 1415 (1970); Can. J. Phys. **48,** 3021 (1970); J. C. Kimball and R. W. Stark, Phys. Rev. B **4,** 1786 (1971).

[17]J. A. Munarin, J. A. Marcus, and P. E. Bloomfield, Phys. Rev. **172,** 718 (1968).

[18]W. A. Reed, Phys. Rev. **188,** 1184 (1969).

[19]The actual phase difference between the incident and transmitted fields for a sample thickness L is given by $\phi'(H) = \phi_0 + [(\omega \pm \omega_c)/\langle v_H\rangle]L$, where ϕ_0 is a phase angle introduced in the skin-depth layer. Experiments have shown ϕ_0 to be relatively independent of H except near cyclotron resonance (Ref. 9).

[20]T. G. Phillips, G. A. Baraff, and P. H. Schmidt, Phys. Rev. Lett. **25,** 930 (1970).

[21]G. A. Baraff and T. G. Phillips, Phys. Rev. Lett. **24,** 1428 (1970).

[22]P. R. Antoniewicz, Phys. Rev. **185,** 863 (1969).

[23]D. S. Falk, B. Gerson, and J. F. Carolan, Phys. Rev. B **1,** 406 (1970).

[24]A. W. Overhauser and S. Rodriguez, Phys. Rev. **141,** 431 (1966).

[25]The odd harmonics only occur in a transmission experiment. In a reflection experiment, the electron must return to the first surface to produce a signal and only the even harmonics are present.

[26]The thickness dependence is in agreement with that found by Falk *et al.* (Ref. 23) in the limit $\omega \ll \omega_c$ and $\lambda < L$. They find for limiting-point resonances a L^{-2} dependence and for extremal helical-trajectory resonances a $L^{-(3/2)}$ dependence.

[27]G. A. Baraff, Phys. Rev. **167,** 625 (1968).

[28]R. F. Milligan and T. G. Castner, Phys. Rev. Lett. **26,** 1560 (1971).

[29]R. B. Lewis and T. R. Carver, Phys. Rev. **155,** 309 (1967).

[30]P. Monod and S. Schultz, Phys. Rev. **173,** 645 (1968).

[31]With our homodyne detection, the leakage just causes a zero off set on the lock-in amplifier. For superheterodyne detection, leakage of this magnitude would probably saturate the if amplifiers.

[32]M. Yaqub and J. F. Cochran, Phys. Rev. **137,** A1182 (1965).

[33]It should be noted that the geometries of the two experiments are not the same. For the dc data $\vec{H}$ was rotated in a plane perpendicular to the current direction while for the present experiment $\vec{H}$ was rotated in a plane containing $\vec{j}$.

[34]V. F. Gantmakher and E. A. Kaner, Zh. Eksp. Teor. Fiz. **45,** 1430 (1963) [Sov. Phys.-JETP **18,** 988 (1964)].

[35]R. J. von Gutfeld and A. H. Nethercot, Phys. Rev. Lett. **18,** 855 (1967).